A SEARCH FOR LEPTONIC PHOTON, Z_l, AT ALL THREE CLIC ENERGY STAGES BY USING ARTIFICIAL NEURAL NETWORKS (ANN)*

S.O. Kara

Niğde Ömer Halisdemir University, Bor Vocational School
51240, Niğde, Turkiye
seyitokankara@gmail.com

S. Akkoyun

Cumhuriyet University, Faculty of Sciences, Department of Physics
58140, Sivas, Turkiye
sakkoyun@cumhuriyet.edu.tr

Received 4 December 2023, accepted 14 June 2024,
published online 1 July 2024

In this work, the possible dynamics of the massive leptonic photon Z_l are reconsidered via the $e^+e^- \to \mu^+\mu^-$ process at the Compact Linear Collider (CLIC) with the updated center-of-mass energies (380, 1500, and 3000 GeV). We show that new generation colliders as CLIC can observe the massive leptophilic vector boson Z_l with mass up to the center-of-mass energy, provided that the leptonic coupling constant is $g_l \geq 10^{-3}$. In this study, we also estimated the cross sections by artificial neural networks using the theoretical results we obtained for CLIC. According to the results obtained, it was seen that these predictions could be made through machine learning.

DOI:10.5506/APhysPolB.55.6-A4

1. Introduction

The idea of the massless leptonic vector particle was first proposed by Okun [1]. Experiments testing the equality of inertial and gravitational masses [2] have put a very strong limit on the interaction constant of the massless leptonic photon with matter $\alpha_l < 10^{-49}$. When this constant is compared to the electromagnetic interaction constant ($\alpha_{\mathrm{EM}} \approx 10^{-2}$), it is natural to conclude that massless leptonic photons coupled to the lepton charge do not exist. However, the use of an extra range for the leptonic interaction constant [3] has revived interest in this subject and led to many publications [4–11].

In [12], it was phenomenologically shown that the lepton charge is coupled to the leptophilic massive vector boson and the possible dynamics is associated with these charges in future linear colliders such as the International Linear Collider (ILC) and the Compact Linear Collider (CLIC). The CLIC is optimized to be built and operated at collision energies of 380, 1500, and 3000 GeV [13]. Many works in the literature have assessed CLICs reach to vector bosons in different contexts [14–20].

In this paper, we have reconsidered phenomenology of the massive leptonic photon, Z_l, at all three CLIC energy stages, using the updated key parameters as in [21]. We also estimated the cross sections by artificial neural networks using the theoretical results we obtained for CLIC. Recently, the ANN method has been applied for the determination of cross sections in high-energy physics. Addepalli [22] has applied machine learning techniques for cross-section measurements for the vector-boson fusion production of the Higgs boson. Mekosh [23] used machine learning to search for the vector-boson scattering at the CMS detector. Sauerburger [24] performed $H \to \tau\tau$ cross-section measurements using machine learning in the ATLAS detector. Akkoyun and Kara [25] did an approximation to the cross sections of the Z_l boson production at CLIC by using neural networks. Kara *et al.* [26] used the neural network method in order to investigate the leptophilic gauge boson Z_l at ILC. In the present study, we used ANN to make some predictions of cross sections. According to the results obtained, it was seen that these predictions could be made through the machine learning. In Section 2, the model is formulated and the artificial neural network (ANN) has been explained. Production of the Z_l boson at the CLIC energy stages is analyzed in Section 3. In Section 4, the ANN results are presented. The results obtained are summarized in the final section.

2. Material and methods

2.1. The model

In our model, to gauge the leptonic quantum number a new $\mathrm{U}_l'(1)$ global Abelian symmetry is added to Standard Model (SM) gauge group $(\mathrm{SU}_C(3) \times \mathrm{SU}_W(2) \times \mathrm{U}_Y(1))$. With the experimental discovery of neutrino oscillations [27], the idea of individually conserving electron, muon, and tau-lepton charges is invalidated. Therefore, we consider a single-lepton charge which is the same for e, μ, τ, and corresponding neutrinos. We also introduce for the interaction of the electroweak vector bosons with fermions, the following replacement in the free fields Lagrangian:

$$\partial_\mu \to D_\mu = \partial_\mu - ig_2 \boldsymbol{T} \cdot \boldsymbol{A}_\mu - ig_1 \frac{Y}{2} B_\mu - ig_l a_l B'_\mu \,, \tag{1}$$

where g_2, g_1, and g_l are interaction constants, $\boldsymbol{T}$ is an isospin operator of a corresponding multiplet of fermionic or Higgs fields, Y is hypercharge, and a_l is the lepton charge of the corresponding multiplet, $\boldsymbol{A}_\mu$, B_μ, B'_μ are gauge fields. A mechanism is needed to provide mass to the leptophilic Z_l vector boson that coincides with the B'_μ vector field. Therefore, the Higgs field with a lepton charge must be added to the model. The interaction Lagrangian, obeying the $\mathrm{SU}_C(3) \times \mathrm{SU}_W(2) \times \mathrm{U}_Y(1) \times \mathrm{U}'_l(1)$ gauge symmetry, can be decomposed as

$$L = L_{\mathrm{SM}} + L' \,, \tag{2}$$

where L_{SM} is the Standard Model Lagrangian and L' is given by

$$L' = \frac{1}{4} F'_{\mu\nu} F^{\mu\nu\prime} + g_l J^\mu_{\mathrm{lep}} B'_\mu + (D_\mu \Phi)^\dagger (D_\mu \Phi) + \mu^2 |\Phi|^2 - \lambda |\Phi|^4 \,, \tag{3}$$

where

$$F'_{\mu\nu} = \partial_\mu B'_\nu - \partial_\nu B'_\mu \tag{4}$$

is the field strength tensor and

$$J^\mu_{\mathrm{lep}} = \Sigma_l a_l \left[\overline{\nu_l} \gamma^\mu \nu_l + \bar{l} \gamma^\mu l \right] \tag{5}$$

is the leptonic current interacting with leptopfilic Z_l, Φ is the singlet complex scalar Higgs field.

2.2. Artificial Neural Network (ANN)

The ANN method is one of the alternative strong tools for the physics problems [28]. It mimics the brain functionality and nervous system. ANN, which is the base of artificial intelligence, can learn the structure of the data and the relationship between them using appropriate algorithms. ANN is composed of mainly three different layers which are the input, hidden, and output layers. Each layer includes its own neurons. The data is taken from the outside by the input layer neurons as inputs and the output data is the desired one which is exported from the output layer neurons. The number of input neurons depends on the problem. As clearly known, inputs are the independent variables of the problem, outputs are the dependent ones.

The number of output neurons is the number of output variables of the problem. In the input and output layers, there is one or more layers in which data is mainly processed. It is called as a hidden layer and it is crucial for solving non-linear problems. There is no common rule for the determination of the numbers of hidden layera and hidden neurons. These numbers are independent of the problem. In the fully connected feed-forward

ANN model which was used in the present study, data flows in one direction from input to output neurons. Each neuron in the layer is connected to all other neurons in the next layer. Therefore, all hidden and output layer neurons have at least one entry. All the entries to the neurons are multiplied by the weight values of their connections and then summed to get the net inputs of the neurons. After obtaining net input to the neuron, it is activated by an appropriate activation function and the outcome is generated. This information is transmitted to the neurons in the next layer by weighted connections. In the case of the output neurons, the outcome is the solution to the problem. In the ANN calculations, all data belonging to the given problem has been divided into two main separate sets. The first part of the data (75% in the present study) is used for the training of ANN. To see the generalization ability of the method, it must be tested over another set of data which is the test dataset (25% in the present study). The main task in the training is the determination of the values of weighted connections between neurons. In other words, the training process is aimed to find the best weight values which give the best estimation starting from the input. Therefore, the weight values are modified until the acceptable error level between the desired and neural network outputs is reached. Generally, the mean square error function (MSE) has been used for the calculation of the error level. In order to reach the best weight values, some parameters such as the hidden layer number, hidden neuron number, learning algorithm, activation function, and/or kind of neural network in the training stage are tuned up.

In this study, to get the best values, one hidden layer with 4, 7, and 10 neurons, the Levenberg–Marquardt learning algorithm, tangent hyperbolic activation function, and multi-layer feed-forward neural network have been used. By using final weights values, the comparison has been made between the neural network outputs and the desired values. The inputs were g_l, M_{Z_l}, and energy for the estimation of the cross section. Of the total 412 data available for 380 GeV, 1.5 TeV, and 3 TeV energy values, 310 were used in the training stage and 102 were used in the test stage. During the training of the ANN, no other data sharing was performed. However, the results obtained are given separately in Section 4 according to different energy and g_l values. The range of activation function is $(-1;\ 1)$ for the hyperbolic tangent of the hidden layer. Therefore, it can be said that it can potentially be difficult to train cases without normalizing or softening the data. Generally in the method, the data is normalized or smoothed in order to speed up the learning process and increase the learning rate. In this case, data are always positive and their scales vary drastically, one simple way is to use the logarithm transformation of the data. Thus, we have taken the logarithm of the output values in all the calculations.

3. Production of the Z_l boson at the CLIC energy stages

The CLIC has been revised with the updated center-of-mass energies, 380 GeV, 1.5 TeV, 3 TeV, and key parameters for these energy stages. In new generation linear colliders as CLIC, it is very difficult to use the total beam energy for the production cross section of the particles obtained as a result of scattering. For this reason, it is necessary to consider the effects of initial-state radiation (ISR) and beamstrahlung (BS). To account for all these effects, we used the beam design parameters given in Table 1.

Table 1. Key parameters of the CLIC energy stages.

Parameters	Stage 1	Stage 2	Stage 3
$E\,(\sqrt{s}\,)$ GeV	380	1500	3000
$L\ \left[10^{34}\,\mathrm{cm}^{-2}\,\mathrm{s}^{-1}\right]$	1.5	3.7	6.0
$N\ \left(10^{9}\right)$	5.2	3.7	3.7
σ_x [nm]	149	60	40
σ_y [nm]	3	1.5	1
σ_z [μm]	70	44	44

Here, E is the center-of-mass energy, L is the luminosity, N is the number of particles in the bunch, σ_x and σ_y are RMS transverse beam sizes at Interaction Points (IP), and σ_z is the RMS bunch length.

After designing the model in Section 2, we implement Lagrangian (3) into the CALCHEP Simulation Program [29] for numerical calculations.

Before proceeding to the calculations, it is necessary to determine the parameter space of the model introduced above. In [30, 31], the authors get some limits from the sensitive electroweak data on different kinds of Z' bosons. In our calculations, we prefer the limit value from [30]

$$\frac{M_{Z_l}}{g_l} \geq 7\ \mathrm{TeV}\,. \tag{6}$$

As seen in Table 2, the upper bounds of interaction constants for different mass values of Z' obey condition (6). The mass-to-coupling ratio is crucial for understanding the properties of the leptonic photon and the nature of this possible new interaction.

In all the calculations, we have determined the signal process as $e^+e^- \to \gamma$, $Z, Z_l \to \mu^+\mu^-$ and the background process as $e^+e^- \to \gamma, Z \to \mu^+\mu^-$. We have chosen this process as the final state containing the e^+e^- pair has a huge background (*i.e.* due to Bhabha scattering). Also, the $\tau^+\tau^-$ pair causes complications in the signal due to τ decays; it is an unobservable $\overline{\nu}\nu$ pair in the final state. Figure 1 (a), (b), and (c) show the cross section *versus* mass

Table 2. Upper bounds of g_l for different values of Z_l mass.

M_{Z_l} [TeV]	g_l
0.38	0.05
0.5	0.07
1.0	0.14
1.5	0.21
2.0	0.28
2.5	0.35
3.0	0.42

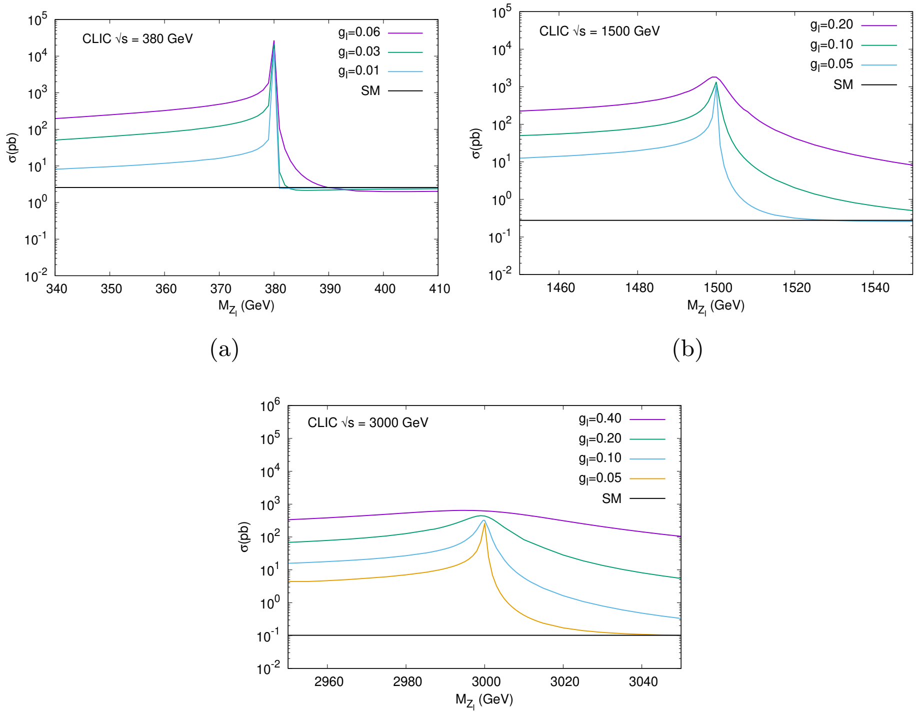

(c)

Fig. 1. Total cross section *versus* mass values of the leptonic photon for different coupling constant values at CLIC with (a) $\sqrt{S} = 380$ GeV, (b) $\sqrt{S} = 1.5$ TeV, and (c) $\sqrt{S} = 3$ TeV.

values of the leptonic photon for different coupling constant values at CLIC with the center-of-mass energies of 380 GeV, 1.5 TeV and 3 TeV, respectively. At all three energy stages, the signal appears to be well above the SM background even for small g_l values. This is due to positive interferences between γ, Z, and Z_l for mass values less than the center of mass energy and for equal and larger values, it is due to the interference of Z_l with γ and Z. In Fig. 1 (c), one can easily see the shift of the cross-section peak from the center-of-mass energy, especially for large values of g_l. This shift is due to ISR and BS effects.

In Fig. 2, the cross section *versus* coupling constant g_l values is plotted to show the effects of ISR and BS together with machine design parameters for CLIC with $\sqrt{S} = 380$ GeV, 1.5 TeV, and 3 TeV. It is clear that these effects reduce the corresponding cross-sections at $M_{Z_l} \approx \sqrt{S}$, especially for lower values of g_l. Figure 2 presents that ISR and BS effects are more efficient at higher energies: the reduction factors for $g_l = 0.05$ are 7 and 12 at $\sqrt{S} = 380$ GeV and 3 TeV, respectively. The following cuts $|M_{\rm inv}(\mu^+\mu^-) - M_{Z_l}| < 10$ GeV and $|\eta_\mu| < 2$ have been used to determine the discovery potential of CLIC at all three energy stages.

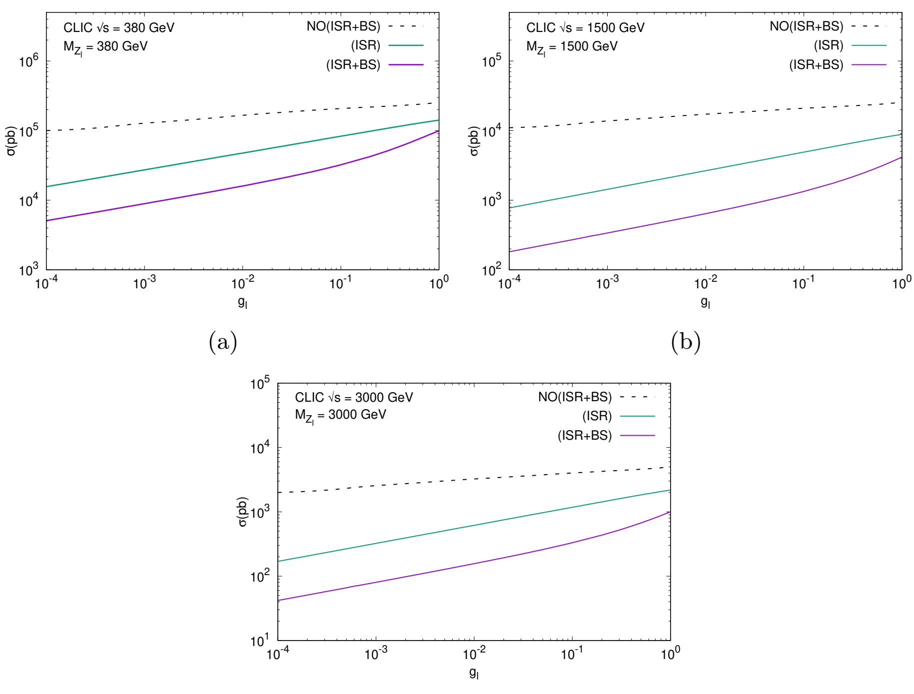

(a) (b)

(c)

Fig. 2. The effects of ISR and BS depending on coupling constant g_l for CLIC with (a) $\sqrt{S} = 380$ GeV, (b) $\sqrt{S} = 1.5$ TeV, and (c) $\sqrt{S} = 3$ TeV.

Statistical significance (S) is calculated using the following formula:

$$S = \frac{\sigma_{\text{signal}} - \sigma_{\text{SM}}}{\sqrt{\sigma_{\text{SM}}}} \sqrt{L_{\text{int}}}\,, \tag{7}$$

where σ_{signal} and σ_{SM} are the cross section of signal and background, respectively, and L_{int} is the luminosity of the interaction. 3σ observations and 5σ discovery contours against M_{Z_l} and g_l for CLIC (380, 1500, and 3000 GeV) are shown in Fig. 3. As can be seen from Fig. 3 (a), CLIC with $\sqrt{S} = 380$ GeV will give an opportunity for massive leptonic photon, Z_l, searches in the region from 100 GeV to 400 GeV, where the interaction constant is down to $g_l \approx 10^{-3}$. Figures 3 (b) and (c) present similar plots for CLIC with $\sqrt{S} = 1.5$ and 3 TeV, respectively. It is seen from Fig. 3 (c) that Z_l could be covered up to $M_{Z_l} = 3$ TeV of $g_l \geq 10^{-3}$ for CLIC $\sqrt{S} = 3$ TeV.

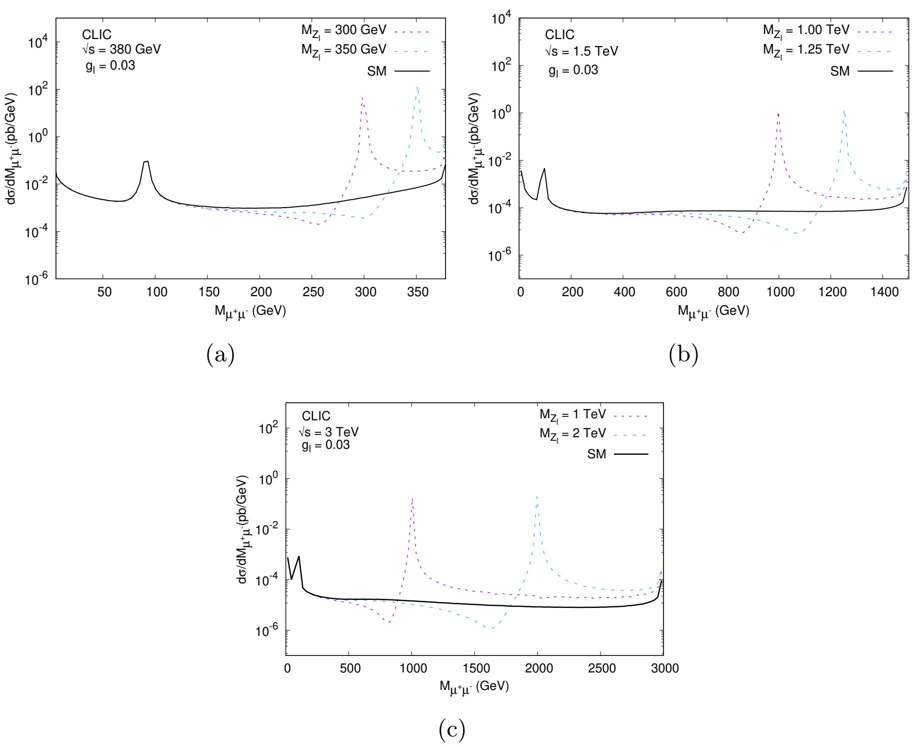

Fig. 3. Achievable limits (for 3σ observations and 5σ discovery) for the mass and coupling parameters at CLIC with (a) $\sqrt{S} = 380$ GeV, (b) $\sqrt{S} = 1.5$ TeV, and (c) $\sqrt{S} = 3$ TeV.

In Figs. 4 (a)–(c), the invariant mass distributions of final muons are plotted for signal and SM background at CLIC ($\sqrt{S}$ = 380 GeV, 1.5 TeV, and 3 TeV). It is clear that the signal is well above the background. As can also be clearly seen from these figures, condition (6) is satisfied.

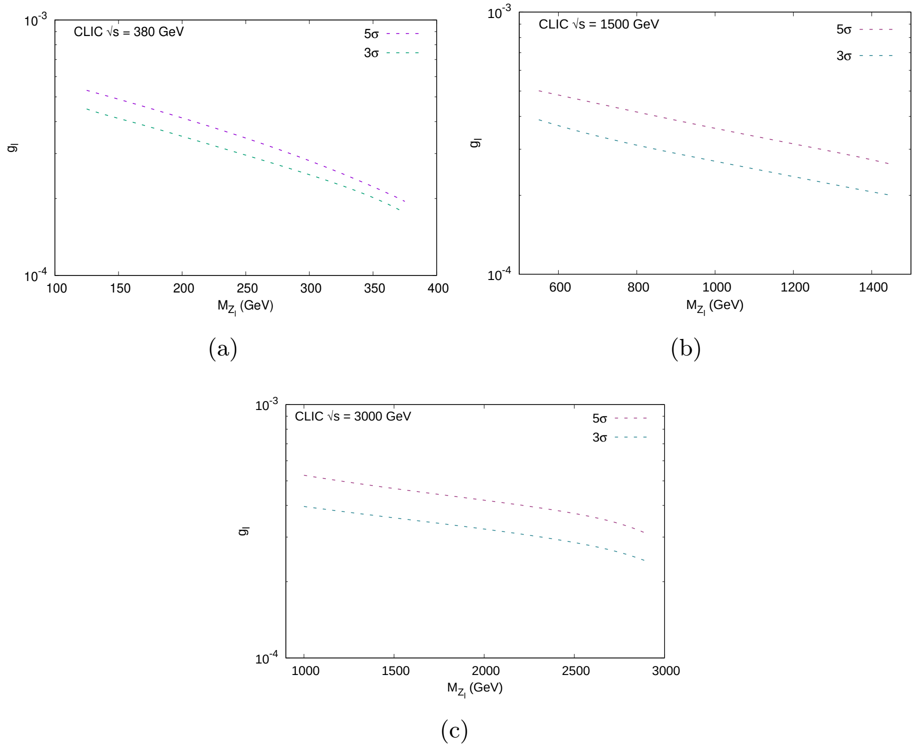

Fig. 4. Invariant mass distributions of final muon pairs for signal and SM background at CLIC with (a) $\sqrt{S} = 380$ GeV, (b) $\sqrt{S} = 1.5$ TeV, and (c) $\sqrt{S} = 3$ TeV (for two different values of M_{Z_l}).

4. Predictions by ANN

ANN calculations performed to obtain influence sections were first tested on the training data set. In Figs. 5–7, the predictions of ANN on this data set are presented separately, according to different energy and g_l values, in comparison with theoretical values. When the results given for 380 GeV in Fig. 5 are examined, it is seen that the ANN structure with $h = 7$ hidden neurons gives more successful results. As can be clearly seen from the graphs, while all three ANN structures are compatible with theoretical data in the high-energy region, the ANN with $h = 4$ and $h = 10$ structures are relatively

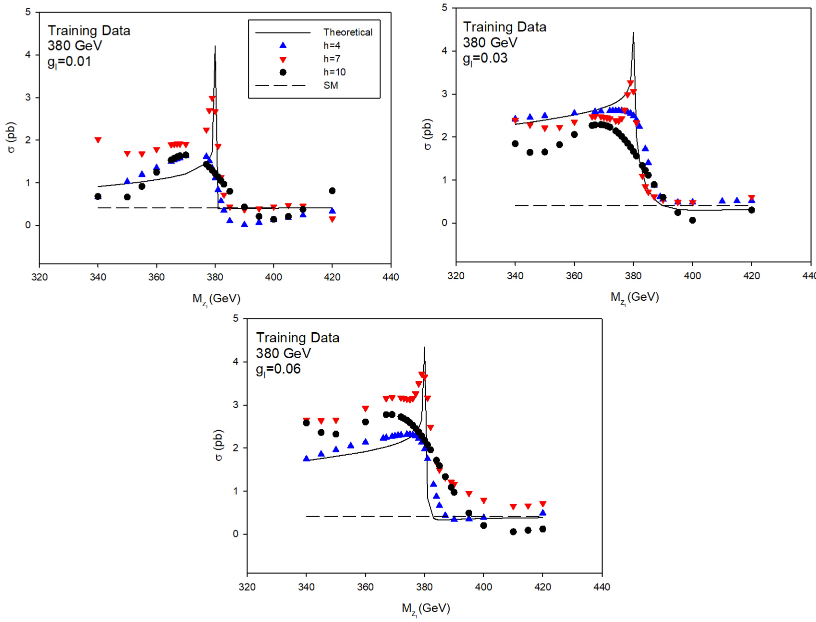

Fig. 5. Estimations of the ANN on the cross sections for $g_l = 0.01$ (top left), $g_l = 0.03$ (top right), and $g_l = 0.06$ (bottom) in 380 GeV.

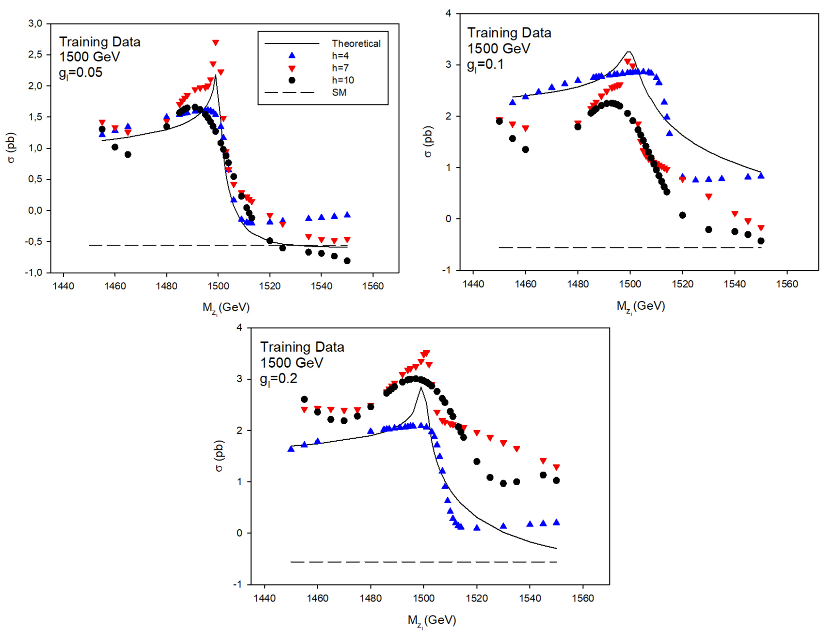

Fig. 6. Estimations of the ANN on the cross sections for $g_l = 0.05$ (top left), $g_l = 0.1$ (top right), and $g_l = 0.2$ (bottom) in 1.5 TeV.

closer to the theoretical values at low energies. However, results compatible with the peak at 380 GeV were obtained with the $h = 7$ ANN structure. When Fig. 6 is examined, results of 1.5 TeV energy values are given for different g_l values. At this energy value, it is clearly seen that the $h = 7$ ANN structure is successful in capturing the peak in the cross section. Finally, in Fig. 7, the prediction results for 3 TeV are presented. The sudden increase in the peak could be achieved with the $h = 7$ ANN structure. In the high- and low-energy regions, it is seen that the ANN structure with $h = 4$ is more successful.

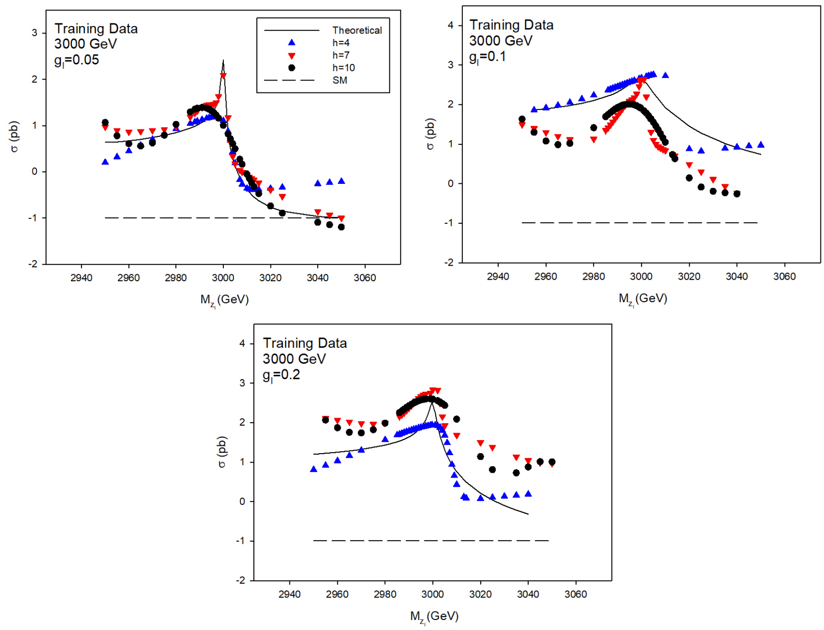

Fig. 7. Estimations of the ANN on the cross sections for $g_l = 0.05$ (top left), $g_l = 0.1$ (top right), and $g_l = 0.2$ (bottom) in 3 TeV.

The prediction results of ANN calculations on test data are given in Figs. 8–10 in comparison with theoretical results. In the figures, the differences between the results of the calculations for 380 GeV, 1.5 TeV, and 3 TeV from the theoretical values are shown, respectively. For 380 GeV, the $h = 10$ structure in the case of $g_l = 0.01$, the $h = 4$ structure in the case of $g_l = 0.03$, and the $h = 4$ structure in the case of $g_l = 0.06$ generally made more successful predictions. When the graphs for 1.5 TeV are examined, it is clear that the $h = 4$ structure for $g_l = 0.05$ and $g_l = 0.1$ and the $h = 10$ structure for $g_l = 0.2$ give more successful results compared to the others. For the 3 TeV energy value, ANN with the $h = 4$ structure for $g_l = 0.05$ and ANN with the $h = 10$ structure for $g_l = 0.1$ and $g_l = 0.2$ made better predictions.

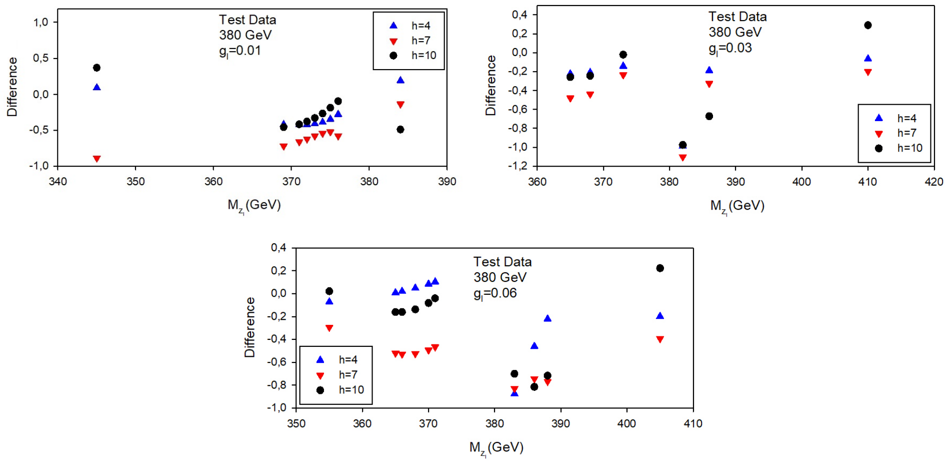

Fig. 8. Test dataset predictions of the ANN on the cross sections for $g_l = 0.01$ (top left), $g_l = 0.03$ (top right), and $g_l = 0.06$ (bottom) in 380 GeV.

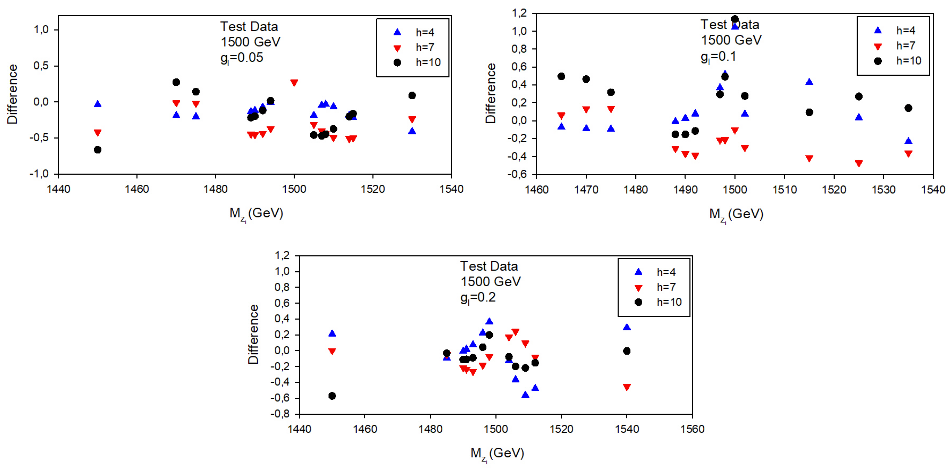

Fig. 9. Test dataset predictions of the ANN on the cross sections for $g_l = 0.05$ (top left), $g_l = 0.1$ (top right), and $g_l = 0.2$ (bottom) in 1.5 TeV.

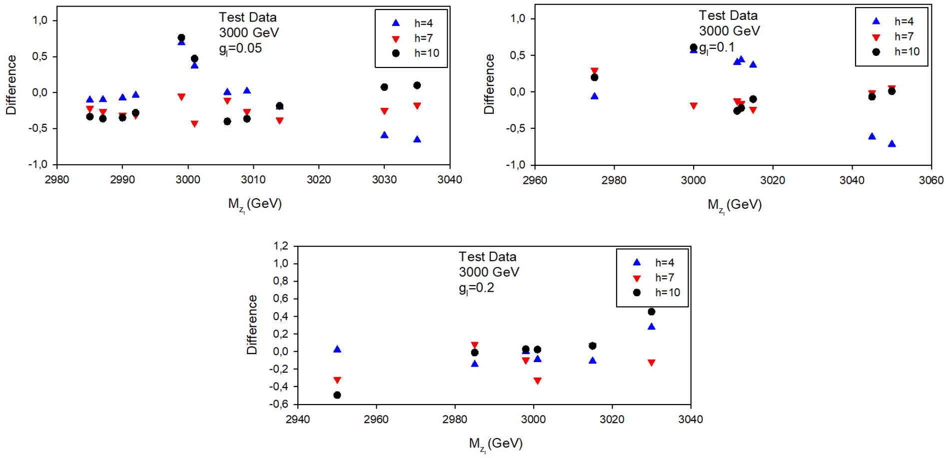

Fig. 10. Test dataset predictions of the ANN on the cross sections for $g_l = 0.05$ (top left), $g_l = 0.1$ (top right), and $g_l = 0.2$ (bottom) in 3 TeV.

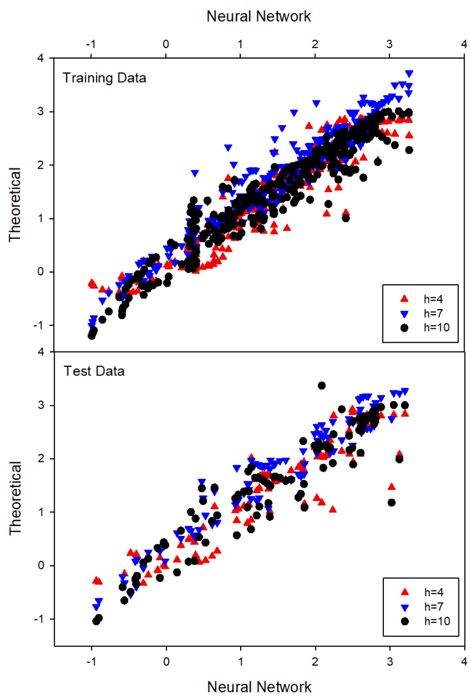

Fig. 11. ANN estimation *versus* theoretical values for training dataset (top) and test dataset (bottom) for different ANN structures.

In Fig. 11, graphs of ANN predictions on the training and test data sets compared to theoretical results are presented separately. When the scatter plot of the training data set is examined, it is seen that the distribution for $h = 10$ is narrower, while the others are relatively more widespread. When the distributions of the test data set were examined, it was seen that the $h = 4$ ANN structure showed a less widespread distribution.

5. Conclusions

In this paper, we have shown that the massive leptonic vector boson, Z_l, with masses up to the center-of-mass energy can be observed using the $e^+e^-\to\mu^+\mu^-$ process at new generation linear collider CLIC with the updated center-of-mass energies ($\sqrt{S} = 380$ GeV, 1.5 TeV, and 3 TeV) and machine design parameters, provided that $g_l \geq 10^{-3}$. This study presents hypotheses regarding some fundamental properties, such as mass and coupling constant, of a possible new massive vector boson, Z_l. From the calculations and the results, it can be concluded that ISR and BS will have a significant impact on the investigation of Z_l at CLIC. At the higher center-of-mass energy such as CLIC with $\sqrt{S} = 3$ TeV, this impact becomes more important. When the results obtained in ANN calculations were examined, it was seen that the ANN structure with 10 hidden layer neurons ($h = 10$) was more successful in the training phase, and the structure with 4 hidden layer neurons ($h = 4$) was more successful in the testing phase. However, the ANN structure with 7 hidden layer neurons ($h = 7$) was more successful in more accurately predicting the peaks corresponding to the sudden increase in the cross sections. As a result, it is concluded that ANN can be used as an alternative tool for estimating influence sections.

REFERENCES

[1] L.B. Okun, «On muonic charge and muonic photons», *Yad. Fiz.* **10**, 358 (1969), [*Sov. J. Nucl. Phys.* **10**, 206 (1969)].

[2] R.V. Eötvös, D. Pekár, E. Fekete, «Beiträge zum Gesetze der Proportionalität von Trägheit und Gravität», *Ann. Phys.* **373**, 11 (1922).

[3] A.K. Çiftçi, S. Sultansoy, Ş. Türköz, «Compensation of lepton charge of matter with relic anti-sneutrinos», *Phys. Lett. B* **355**, 494 (1995).

[4] L. Okun, «Leptons and photons», *Phys. Lett. B* **382**, 389 (1996), arXiv:hep-ph/9512436.

[5] L.B. Okun, «Leptonic Photon and Light Element Abundancies», *Mod. Phys. Lett. A* **11**, 3041 (1996), arXiv:hep-ph/9611360.

[6] B.V. Martemyanov, «On the thickness of the skin layer for screening of the leptonic charge of a body», *JETP Lett.* **66**, 547 (1997).

[7] S.N. Gninenko, «Limit on leptonic photon interactions from SN1987a», *Phys. Lett. B* **413**, 365 (1997), arXiv:hep-ph/9708465.

[8] V.A. Ilyin, L.B. Okun, A.N. Rozanov, «On the search for muonic photons in neutrino experiments», *Nucl. Phys. B* **525**, 51 (1998), arXiv:hep-ph/9707479.

[9] CHARM II Collaboration (P. Vilain *et al.*), «Experimental search for muonic photons», *Phys. Lett. B* **434**, 200 (1998).

[10] A.D. Dolgov, «Long-range forces in the universe», *Phys. Rep.* **320**, 1 (1999).

[11] J.W. Brockway, «Another look at leptonic photon couplings», *Phys. Lett. B* **682**, 342 (2010).

[12] S.O. Kara, M. Sahin, S. Sultansoy, S. Turkoz, «A search for leptophilic Z_l boson at future linear colliders», *J. High Energy Phys.* **2011**, 072 (2011).

[13] CLIC, CLICdp collaborations, «Updated baseline for a staged Compact Linear Collider», CERN2016-004, 2016.

[14] Xin Qin, Jie-Fen Shen, «Search for single production of vector-like B quark decaying to a Higgs boson and bottom quark at the CLIC», *Nucl. Phys. B* **966**, 115388 (2021).

[15] C. Callender, A.R. Zerwekh, «A dark vector resonance at CLIC», *Chinese Phys. C* **43**, 063102 (2019).

[16] G. Kačarević *et al.*, «Measurement of the Higgs boson branching ratio BR($H \to \gamma\gamma$) at a 3 TeV CLIC», *Phys. Rev. D* **105**, 092009 (2022).

[17] Chong-Xing Yue, Hua-Ying Zhang, Han Wang, «Production of axion-like particles via vector boson fusion at future electron-positron colliders», *Eur. Phys. J. C* **82**, 88 (2022).

[18] A.A. Billur, M. Köksal, A. Gutierrez-Rodriguez, M.A. Hernandez-Ruiz, «Model-independent limits for anomalous triple gauge bosons $W^+W^-\gamma$ couplings at the CLIC», *Eur. Phys. J. Plus* **136**, 697 (2021).

[19] C. Fleper, W. Kilian, J. Reuter, M. Sekulla, «Scattering of W and Z bosons at high-energy lepton colliders», *Eur. Phys. J. C* **77**, 120 (2017).

[20] O. Karadeniz, A. Şenol, K.Y. Oyulmaz, H. Denizli, «CP-violating Higgs-gauge boson couplings in $H\nu\bar{\nu}$ production at three energy stages of CLIC», *Eur. Phys. J. C* **80**, 229 (2020).

[21] F. Bordry *et al.*, «Machine Parameters and Projected Luminosity Performance of Proposed Future Colliders at CERN», arXiv:1810.13022 [physics.acc-ph].

[22] S.V. Addepalli, ATL-PHYS-PROC-2023-012.

[23] M. Mekosh, Master of Science Thesis, Northern Illinois University De Kalb, Illinois, 2023.

[24] F. Sauerburger, Thesis, Albert-Ludwigs-Universität Freiburg, 2022.

[25] S. Akkoyun, S.O. Kara, «An approximation to the cross sections of Z_l boson production at CLIC by using neural networks», *Centr. Eur. J. Phys.* **11**, 345 (2013).

[26] S.O. Kara, S. Akkoyun, T. Bayram, «Probing for leptophilic gauge boson Z_l at ILC with $\sqrt{s} = 1$ TeV by using ANN», *Int. J. Mod. Phys. A* **29**, 1450171 (2014).

[27] Particle Data Group (K. Nakamura *et al.*), «Review of Particle Physics», *J. Phys. G: Nucl. Part. Phys.* **37**, 075021 (2010).

[28] S. Haykin, «Neural Networks and Learning Machines», *Prentice-Hall Inc.*, Englewood Cliffs, NJ, USA 1999.

[29] A. Pukhov *et al.*, «CompHEP — a package for evaluation of Feynman diagrams and integration over multi-particle phase space. User's manual for version 33», arXiv:hep-ph/9908288.

[30] G. Cacciapaglia, C. Csáki, G. Marandella, A. Strumia, «The minimal set of electroweak precision parameters», *Phys. Rev. D* **74**, 033011 (2006), arXiv:hep-ph/0604111.

[31] F. del Aguila, J. de Blas, M. Pérez-Victoria, «Electroweak limits on general new vector bosons», *J. High Energy Phys.* **2010**, 033 (2010), arXiv:1005.3998 [hep-ph].